Biomaterials Advances 133 (2022) 112622

Contents lists available at ScienceDirect

Biomaterials Advances

journal homepage: www.elsevier.com/locate/bioadv

Bacteria capture with magnetic nanoparticles modified with cationic carbosilane dendritic systems

Sara Quintana-Sánchez [a,b,c,1], Andrea Barrios-Gumiel [a,b,c,1], Javier Sánchez-Nieves [a,b,c,*], José L. Copa-Patiño [d], F. Javier de la Mata [a,b,c,*], Rafael Gómez [a,b,c]

[a] Dpto. de Química Orgánica y Química Inorgánica, Universidad de Alcalá (UAH); Instituto de Investigación Química "Andrés M. del Río" (IQAR), Universidad de Alcalá (UAH); Alcalá de Henares (Madrid), Spain
[b] Networking Research Center for Bioengineering, Biomaterials and Nanomedicine (CIBER-BBN), Madrid, Spain
[c] Instituto Ramón y Cajal de Investigación Sanitaria, IRYCIS, Madrid, Spain
[d] Dpto. de Biomedicina y Biotecnología, Universidad de Alcalá (UAH), Alcalá de Henares (Madrid), Spain

ARTICLE INFO

Keywords:
Water purification
Magnetic nanoparticles
Bacteria
Dendrimer and dendron
Carbosilane

ABSTRACT

Bacteria elimination from water sources is key to obtain drinkable water. Hence, the design of systems with ability to interact with bacteria and remove them from water is an attractive proposal. A diversity of polycationic macromolecules has shown bactericide properties, due to interactions with bacteria membranes. In this work, we have grafted cationic carbosilane (CBS) dendrons and dendrimers on the surface of iron oxide magnetic nanoparticles (MNP), leading to NP (ca. 10 nm) that interact with bacteria by covering bacteria membrane. Application of an external magnetic field removes MNP from solution sweeping bacteria attached to them. The interaction of the MNP with Gram-positive *S. aureus* bacteria is more sensible to the size of dendritic system covering the MNP, whereas interaction with Gram-negative *E. coli* bacteria is more sensible to the density of cationic groups. Over 500 ppm of NPM, MNP covered with dendrons captured over 90% of both type of bacteria, whereas MNP covered with dendrimers were only able to capture *S. aureus* bacteria (over 90%) but not *E. coli* bacteria. Modified MNP were characterized by transmission electron microscopy (TEM), thermogravimetric analysis (TGA), Fourier-transform infrared spectroscopy (FTIR), Z potential and dynamic light scattering (DLS). Interaction with bacteria was analyzed by UV, TEM and scanning electron microscopy (SEM). Moreover, the possibility to recycle cationic dendronized MNP was explored.

1. Introduction

Bacteria are ubiquitous microorganism with irreplaceable functions for life, including human beings. On the other hand, they are also responsible of severe diseases. High quality drinkable water is critical to avoid infectious diseases and still is one of the main health problems in underdeveloped countries. According to United Nation Organization (UNO), three in ten people lack access to safely managed drinking water services [1]. In developed countries, pollution of spring water related with animal farm is becoming a concern and for travelers in remote regions the access to drinkable water becomes a challenge [2,3]. Hence, bacteria elimination from water is of paramount interest and the design of systems with ability to interact with bacteria and remove them from water is a very attractive proposal.

Nanotechnology is becoming part of the solution creating materials that facilitate the combination of multiple treatments [4]. Among them, nanoparticles stand out as a promising area of research for water purification due to properties such as large surface-to-volume ratio and the possibility to be modified with a rich variety of active functions [5]. Particularly, magnetic nanoparticles (MNP) are being extensively explored due to their susceptibility to be guide by an external magnetic field [6] and due to the variation of properties depending on MNP environment, becoming very interesting in many applications [7–10], including extraction and purification of biomolecules [11,12] or water purification [13]. These magnetic particles are commonly based on magnetite (Fe_3O_4). However, these MNP tend to aggregate forming large nanoclusters, decreasing dispersibility and magnetization, which limit their applications. By functionalization, is possible to reduce this phenomenon and achieve desirable dispersibility in liquid medium, as for example water [14,15].

Regarding extraction of pathogens such as virus or bacteria, the choice of NP functionalization is very important to achieve the correct interaction between the MNP and the microorganism [16–19]. Although for bacteria it has been reported the use of naked iron oxide MNP [16], adequate modification seems a more promising procedure for bacteria capture [18–21].

Frequently, the systems employed to cover MNP and generate activity toward bacteria capture contains cationic moieties, since different polycationic macromolecules interact with and penetrate into bacteria walls [22–25]. For the best activity, it is required an adequate hydrophobic/hydrophilic balance.

* Corresponding authors.
E-mail addresses: javier.sancheznieves@uah.es (J. Sánchez-Nieves), javier.delamata@uah.es (F.J. de la Mata).
[1] Both authors contribute equally to this work.

http://dx.doi.org/10.1016/j.msec.2021.112622
Received 9 September 2021; Received in revised form 12 November 2021; Accepted 15 December 2021
Available online 21 December 2021

Polymers not only protect and give functionality to NP, but can increase the number of active sites on the new system, favouring interactions. In this way, dendritic systems (dendrimers and dendrons) have become a very useful tool. These systems can be considered a class of monodisperse polymers with well-defined size and structure and a multivalent molecular surface [26–28]. As has been commented for multicationic polymers, cationic dendrimers also show relevant antimicrobial properties [29–34]. Their synthesis is made step by step and the increase in the number of repetition steps give dendrimers with higher number of functions (generations). While dendrimers are spherical, dendrons contain an additional branch finished with a different function named focal point. Both systems can transfer their activity to materials as NP by anchoring to NP surface. This procedure can be done through one of the multiple functions in dendrimers or through the focal point in dendrons [35–38]. For example, MNP covered with cationic dendritic systems have been tested for bacteria capture [39,40].

As commented above, the hydrophobic/hydrophilic balance is relevant to obtain a suitable antibacterial activity. For carbosilane (CBS) dendrimers, a type of dendrimers [41], the framework provides the hydrophobic region and modification with peripheral cationic ammonium moieties leads to dendritic systems with bactericidal properties, by themselves [42,43] or when incorporated to NP [44–46].

In this work, we have developed MNP grafted with CBS dendritic systems to analyse the ability of the new MNP to capture Gram-positive *S. aureus* and Gram-negative *E. coli* bacteria, taking into account the influence of topology (dendrimer vs. dendron) and generation (number of branching points, two for G2 dendron and three for G3 dendrons, see Fig. 1). The MNP were characterized by transmission electron microscopy (TEM), thermogravimetric analysis (TGA), Fourier-transform infrared spectroscopy (FTIR), Z potential. Interaction with bacteria was studied by UV, TEM and scanning electron microscopy (SEM). Finally, the possibility to recycle cationic dendronized MNP was also explored.

2. Experimental section

2.1. General considerations

All reactions were carried out under inert atmosphere and solvents were purified from appropriate drying agents when necessary. Thiol-ene reactions were carried out employing a HPK 125 W Mercury Lamp from Heraeus Noblelight with maximum energy at 365 nm, in normal glassware under inert atmosphere. Reagents unless otherwise stated, were obtained from commercial sources and used as received. MNP precursors, dendrons $(EtO)_3SiG_n(S\text{-}NMe_3Cl)_m$ (where $n = 2$, $m = 4$ (**1**); $n = 3$, $m = 8$ (**2**) [47]) were synthesized as published. On the other hand, dendrimer $G_1Si(S\text{-}NMe_2)_7(Si(OEt)_3)$ (**3**) [48] and **MNP3** [48] were published elsewhere. NMR spectra were recorded on a Varian Unity VXR-300 (300.13 (^{1}H), 75.47 (^{13}C) MHz) or on a Bruker AV400 (400.13 (^{1}H), 100.60 (^{13}C)).

FTIR analyses were recorded on a Perkin-Elmer SPECTRUM 2000.

Thermogravimetric analyses (TGA) were performed by using a Q500 analyzer from TGA instrument. Dry and pure samples (2–10 mg) were placed into a platinum sample holder under a nitrogen atmosphere. The measurements were recorded from 50 to 900 °C, with heating rate of 10 °C/min.

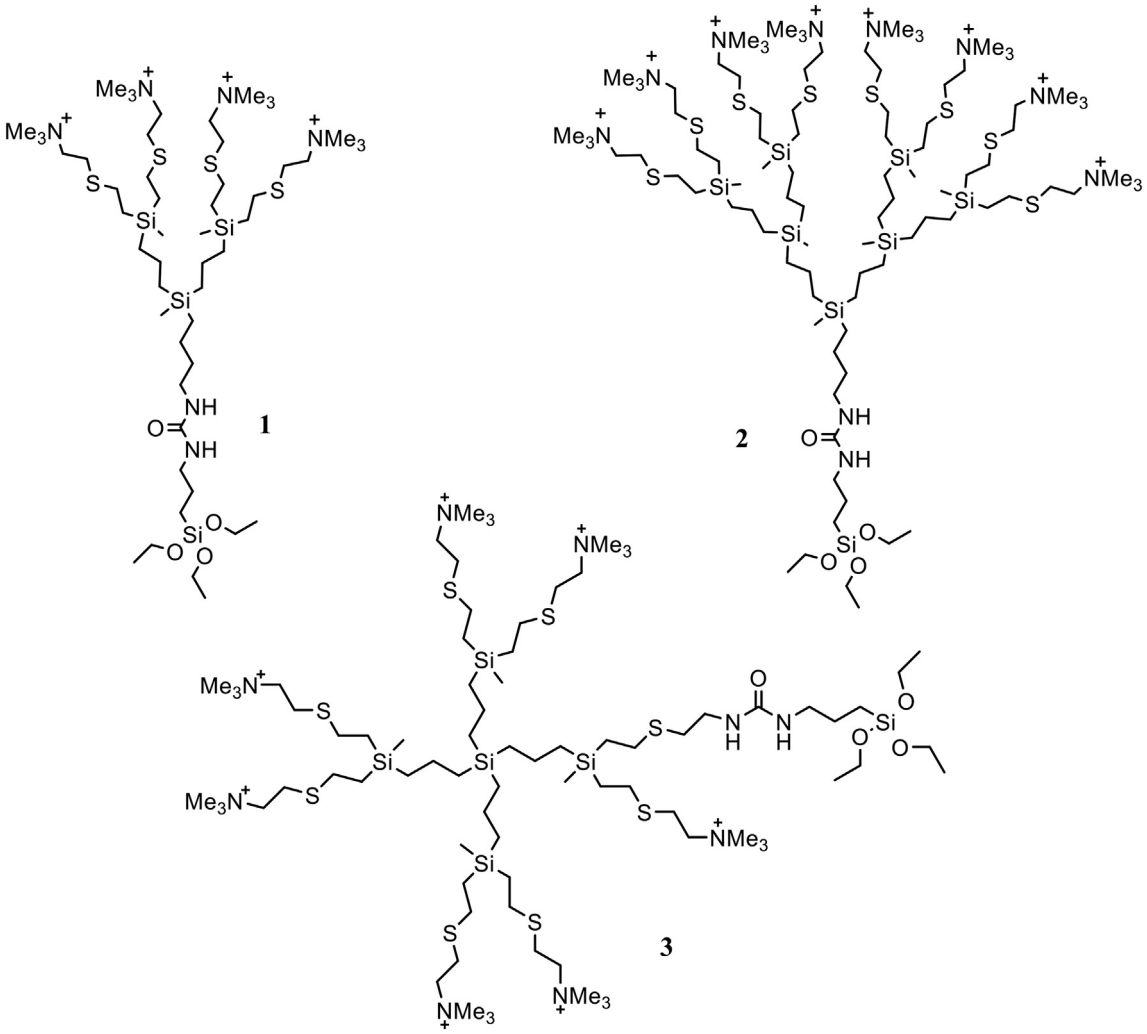

Fig. 1. Structures of cationic CBS dendrons (G2 **1**, G3 **2**) and dendrimers (G1 **3**) employed in this work.

The Z potentials and the hydrodynamic diameter of compounds were measured by Zetasizer Nanno ZS instrument (Malvern Instrument Ltd., UK) at 25 °C in disposable Malvern plastic cuvettes. The solutions were prepared by suspending each compound (0.5 mg) in distilled water (1 ml), which was previously sonicated.

Transmission electron microscopy (TEM) was performed by using a ZEISS EM10 transmission electron microscope with 30 μm lens and a side-mounted 1 K CCD camera, operating at an acceleration voltage of 100 KV with 0.2 nm resolution. The samples were prepared adding a drop of each MNP obtained onto a carbon-coated copper grid (400 mesh). The samples were dried before observation (particle size measurements were performed by using Image J).

2.2. Preparation of Fe_3O_4 MNP

The MNPs (Fe_3O_4) were prepared following the coprecipitation method with minor modifications [49]. A distilled water solution (76 ml) of $FeCl_2{\cdot}4H_2O$ (0.483 g, 2.43 mmol) and $FeCl_3{\cdot}6H_2O$ (1.31 g, 4.86 mmol) were mixed under inert atmosphere with 18 ml of ammonia in water solution (35%), which was added drop by drop with vigorous stirring for 2 h at 90 °C. Then, MNP were obtained and washed two times with distilled water and five times with ethanol, using magnetic decantation or centrifugation to separate the MNP from the supernatant. 0.484 mg of MNP were obtained.

2.3. Surface functionalization of the MNP

MNPs@G_2(S-$NMe_3Cl)_4$ (MNP1). MNP without functionalization were suspended in ethanol (210 ml, 162 mg, 3.33 mM). The suspension was sonicated for 20 min. Then, the CBS dendron $(EtO)_3SiG_2(S\text{-}NMe_3Cl)_4$ (**1**, 0.883 g, 0.699 mmol, molar relationship Fe_3O_4:dendron 1:1), solved in 10 ml of *N*,*N*-dimethylformamide (DMF), was added to the mixture. The reaction mixture was sonicated 10 min more and the mixture was stirred at room temperature for 16 h. The product was secluded and washed five times with distilled water, magnetic decantation or centrifugation to separate the MNP from the supernatant. Then, **MNP1** were dried under vacuum (137 mg). Data for **MNP1**: see Table 1.

MNPs@G_3(S-$NMe_3Cl)_8$ (MNP2). These nanoparticles were prepared following the procedure described previous, from an ethanol suspension of unfunctionalized MNP (Fe_3O_4) (174 ml, 134 mg, 3.33 mM) and a DMF solution of dendron $(EtO)_3SiG_3(S\text{-}NMe_3Cl)_8$ (**2**, 1.35 g, 0.580 mmol, molar relationship Fe_3O_4: dendron 1:1). 104 mg of **MNP2** were obtained. Data for **MNP2**: see Table 1.

2.4. Bacterial assays

2.4.1. Stock solutions of MNP

Stock solutions of MNP coated with cationic carbosilane dendritic systems (**MNP1–3**) and subsequent dilutions were prepared in sterile distilled water. The samples were sonicated for 30 min prior to the assays to avoid agglomeration and to achieve a completely homogeneous sample.

2.4.2. Bacterial capture capacity of cationic MNP at different concentrations

Escherichia coli (CECT 515, Gram-negative bacteria) and *Staphylococcus aureus* (CECT 240, Gram-positive bacteria) were used to evaluate the bacterial capture capacity of MNP. These bacterial strains were obtained from the Spanish Type Culture Collection (CECT).

Suspensions of MNP were prepared in the range of 125 to 4000 ppm in conical tubes to determinate their bacterial capture capacity. Each bacterial suspension, grown for 3 h in Muller Hilton medium, was adjusted to an optical density (OD) of 0.2, at a wavelength of 625 nm. Then, 500 μl of these bacterial suspensions (*E. coli* and *S. aureus*) were added to each suspension of MNP (500 μl). These suspension mixtures were mixed with vortex for 1 min and then were incubated at room temperature for another 10 min. Afterward, bacteria-MNP systems were separated from supernatant by magnetic decantation for 10 min using a magnetic separation rack. OD of this supernatant was then measured. Then, the percentage of bacteria capture was obtained by comparison between OD of supernatant and OD of control (bacteria suspension without treatment):

$$\%\ bacterial\ capture\ \frac{OD_{control} - OD_{supernatant}}{OD_{control}} \times 100$$

The surviving bacteria were determined for bacteria capture and bacteria suspension supernatant. For that, 5 μl of each sample were transferred to plate count agar (PCA, obtained from Scharlau (Spain)) at 37 °C for 20 h.

2.4.3. Capacity of MNP@G_3(S-$NMe_3Cl)_8$ (MNP2) to capture bacteria at different concentrations

Bacterial strains (*E. coli* and *S. aureus*) were grown in 10 ml of Muller-Hilton medium at 37 °C and 150 rpm for 3 h. Then, Muller-Hilton medium was removed by centrifugation and each bacterial strain was resuspended in sterile water until an optical density of 0.08–0.1 at 625 nm (10^8 CFU/ml).

Bacterial suspensions were prepared in the range of 10^3 to 10^8 CFU/ml to determinate the capacity of **MNP2** to capture low concentrations of bacteria. Then, 100 μl of each bacterial suspension were mixed with 900 μl of **MNP2** suspension (500 ppm final concentration). The positive controls were tested on MNP-free wells adding each bacterial suspension in water. Bacteria capture treatment was done following the protocol describe in the previous section. Afterward, bacteria-MNP@$G_3(S\text{-}NMe_3^+)_8$ (**MNP2**) were washed twice with sterile water and re-suspended again in 1 ml of water. The percent of bacterial capture and their viability was determinated by counting colony forming units (CFU). For that, 100 μl of each treatment (bacterial capture, supernatant and controls) were transferred to PCA plate and incubated at 37 °C for 20 h. Higher concentrations of control bacteria were diluted when was needed to count colonies.

2.4.4. MNP@G_3(S-$NMe_3Cl)_8$ (MNP2) recovery and reuse

The evaluation of our capacity to recovery and reuse MNP@$G_3(S\text{-}NMe_3^+)_8$ (**MNP2**) after the first cycle of bacterial capture were studied following different conditions. First of all, the bacteria-**MNP2**, MNP in the range of 250 to 1000 ppm, from the first cycle were washed twice with PBS and then, were directly mixed with new bacterial suspension (10^8 CFU/ml), at the same conditions that in the first cycle were used. This was repeated for 3 cycles. The procedure was analogous to that described above.

In addition, nanoparticles were recovered to be reused, after removing the bacteria previously capture for each cycle. For that, bacteria-**MNP2** were treated with a solution of ethanol/water 75/25 (*v*/v) and sonicated for 5 min to decompose the bacteria cells that were captured. Then, the MNP were decanted by magnetization (10 min in a magnetic separation rack) and the supernatant was removed. Possible ethanol traces were removed washing the **MNP2** twice with sterile water, before doing the next capture cycle.

Percentage of bacteria capture in each cycle for both assays was obtained following the same method than in the first capture cycle.

2.4.5. Study of bacteria-MNP interaction

Images of the interaction between bacteria and our cationic magnetic nanoparticles were obtained through transmission electron microscopy (TEM) and scanning electron microscopy (SEM).

2.4.6. Transmission electron microscopy (TEM)

Bacteria/MNP suspensions, with high yield of capture, were transferred by dropping onto a carbon-coated copper grid (400 mesh). Then, the samples were dried at room temperature before observation by TEM.

2.4.7. Scanning electron microscopy (SEM)

SEM was performed to evaluate the morphology of the *S. aureus* and *E. coli*, when they are captured by MNP. Samples were prepared as follows: 200 μl of poly-L-lysine were used as a coating to enhance bacteria/MNP attachment and adhesion to glass coverslip. After excess of poly-L-lysine was

removed by washed twice with Phosphate-Buffered Saline (PBS) and 50 μl bacteria/MNP suspensions were incubated on each glass coverslips at room temperature, until dried. Milloning's solution containing 2% glutaraldehyde was used to fix bacteria/MNP suspensions completely. Afterwards, bacteria/MNP were washed in Milloning's solution with 0.5% and different solutions with increasing ethanol concentrations were used to dehydrate first our samples. Finally, each glass coverslip was dehydrated with anhydrous acetone. Samples were critical-point dried using a Polaron CPD7501 critical-point drying system, and sputter-coated with 200 Å gold-palladium using a Polaron E5400. Scanning electron microscopy was performed at 5–15 kV in a Zeiss DSM 950 SEM.

3. Results and discussions

3.1. Synthesis and characterization of cationic MNP

A common procedure for the modification of the MNP surface is a reaction between the hydroxyl groups present on their surface and ligands with a triethoxysilyl moiety. In this way, three different CBS dendritic systems functionalized with ammonium groups (-NMe_3^+), to interact with bacteria membrane, and a triethoxysilyl group were chosen and prepared as previously were described in our research group (Fig. 1) [44]. On one side, we have employed two CBS dendrons $(EtO)_3SiG_n(S\text{-}NMe_3^+)_m$ (G2, $n = 2$, m $= 4$ (**1**); G3, $n = 3$, m $= 8$ (**2**)) [44], with the aim to evaluate the influence of the number of cationic groups on the ligand; on the other side, a cationic CBS dendrimer, $G_1Si(S\text{-}NMe_3^+)_7(S\text{-}Si(OEt)_3)$ (G1 **3**) [48], to know how the dendritic morphology could affect to the functionalization of the MNP surface and consequently, in their activity.

Hence, the reaction of the CBS dendritic systems commented above with free Fe_3O_4 MNP (1:1 dendritic system:MNP ratio) in EtOH led to the modified MNP **MNP1–3** (Scheme 1). The MNP were separated from solution by precipitation using an external magnet or by centrifugation. After grafting the dendritic systems on MNP surface, the new **MNP1–3** dispersed better in water, probably due to an electrostatic repulsion between their ammonium groups. These MNP were characterized by TEM, Z potential, DLS, TGA and FTIR (Table 1).

Images obtained by TEM with our functionalized **MNP1–3** showed similar sizes among them as expected coming from the same core, 11 ± 2 nm for **MNP1**, 11 ± 3 nm for **MNP2**, 12 ± 2 nm for **MNP3** (Fig. 2). (See Fig. 3.)

TGA analysis allowed us to study the percentage of organic matter (dendritic system) grafted on the nanoparticle surface. This technique confirmed the modification on each MNP surface. The weight loss for MNP decorated with second (G2) and third (G3) generation dendrons was 10.2% (**MNP1**) and 21.5% (**MNP2**), while for the MNP modified with G1 dendrimer **MNP3**, a weight loss of 6.7% was observed. With these data, the final Fe_3O_4/L molar ratio was calculated (Table 1).

These ratio values are notably different to the Fe_3O_4/L molar ratio employed in the reaction because the majority of the Fe_3O_4 is not accessible, since it belongs to the inner core of the MNP. However, addition of smaller amounts of ligands led also to smaller functionalization degree. Additionally, the number of ligands (that is, number of dendrons or dendrimers) and ammonium functions were calculated from data obtained by TGA and TEM for the different MNP prepared. Functionalization degree of MNP was similar for both MNP covered with dendrons (N_L (**MNP1**) = 224; ρ_L (**MNP2**) = 274), but with dendrimer the functionalization degree was 3 times lower (N_L (**MNP3**) = 83). Regarding the number of functions on the NP surface, this value was higher for **MNP2**, containing G3 dendrons, than for **MNP1**, containing G2 dendrons, due the different generation of dendrons, and consequently, the different number of cationic groups, eight for dendron **2** and four for dendron **1**. In this way, the highest number of cationic groups on the NP surface could be an advantage to capture bacteria. The lower functionalization degree of **MNP3**, covered with G1 dendrimers, with respect to **MNP1–2**, covered with dendrons, can be attributed to the topology of the ligands. The triethoxysilyl moiety in dendrons is located in a longer chain than in dendrimers, sticking out of the dendritic core and then making easier the reaction with the MNP surface.

Z potential measurements (Table 1) supported that dendritic systems were grafted onto MNP surface. Data of bare and dendritic systems coated MNP showed significant differences, being negative for unfunctionalized MNP (−38.6 mV) and clearly positive for modified MNP (+29.1 mV for **MNP1**, +29.7 mV for **MNP2**, +26 mV for **MNP3**).

Analysis obtained by FTIR showed the presence of the magnetite core by the strong stretching absorption band at 581 cm^{-1} corresponding with FeO vibrations. The hydroxyl groups presence in MNP surface are related with the broad band at 3417 cm^{-1} and the band at 1613 cm^{-1}, being attributed to OH stretching and OH bending respectively. In FTIR spectra of MNP functionalized with dendritic systems the band at 1613 cm^{-1} can be overlapped with a characteristic band of urea bond (C=O). The modification of MNP surface was confirmed by the characteristic bands of dendritic systems, 3000–2800 cm^{-1}, as consequence of the ammonium groups (CH_3-N^+) and their hydrocarbon chains (CH_2 and CH_3). Additionally, signal related with Si-OH and Si-O-Fe vibrations can be identified as the band around 997 cm^{-1}.

Since these reactions consumed large amounts of CBS dendritic systems, we explored the recovering of the excess employed. Thus, the first

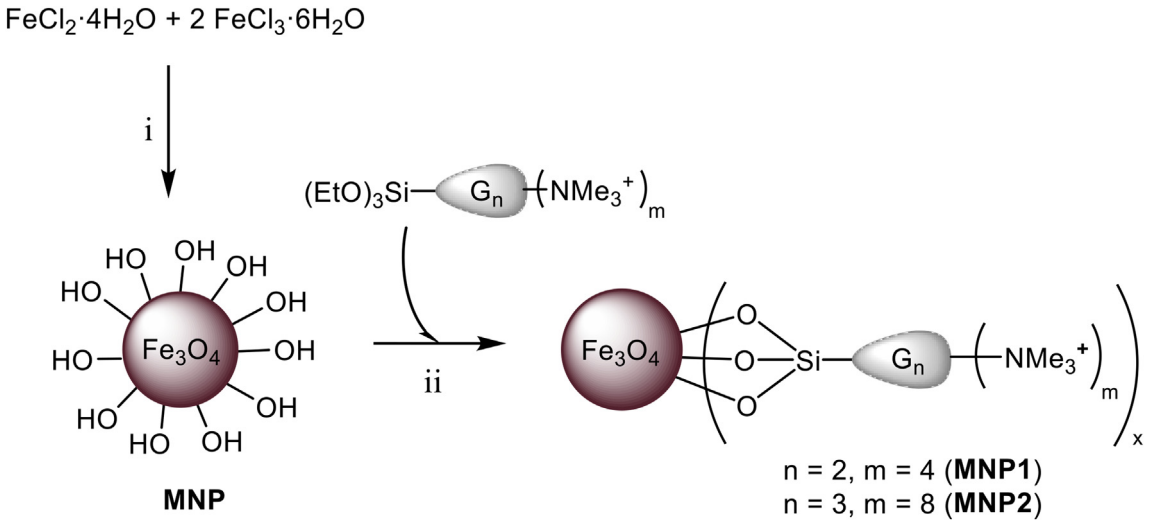

Scheme 1. Synthesis of functionalized MNP with cationic CBS dendrons, **MNP1** ($G_n(S\text{-}NMe_3^+)_m$ ($n = 2$, m $= 4$) and **MNP2** ($n = 3$, m $= 4$). i) H_2O, 90 °C, NH_3, 2 h; ii) EtOH/DMF, r. T., 16 h.

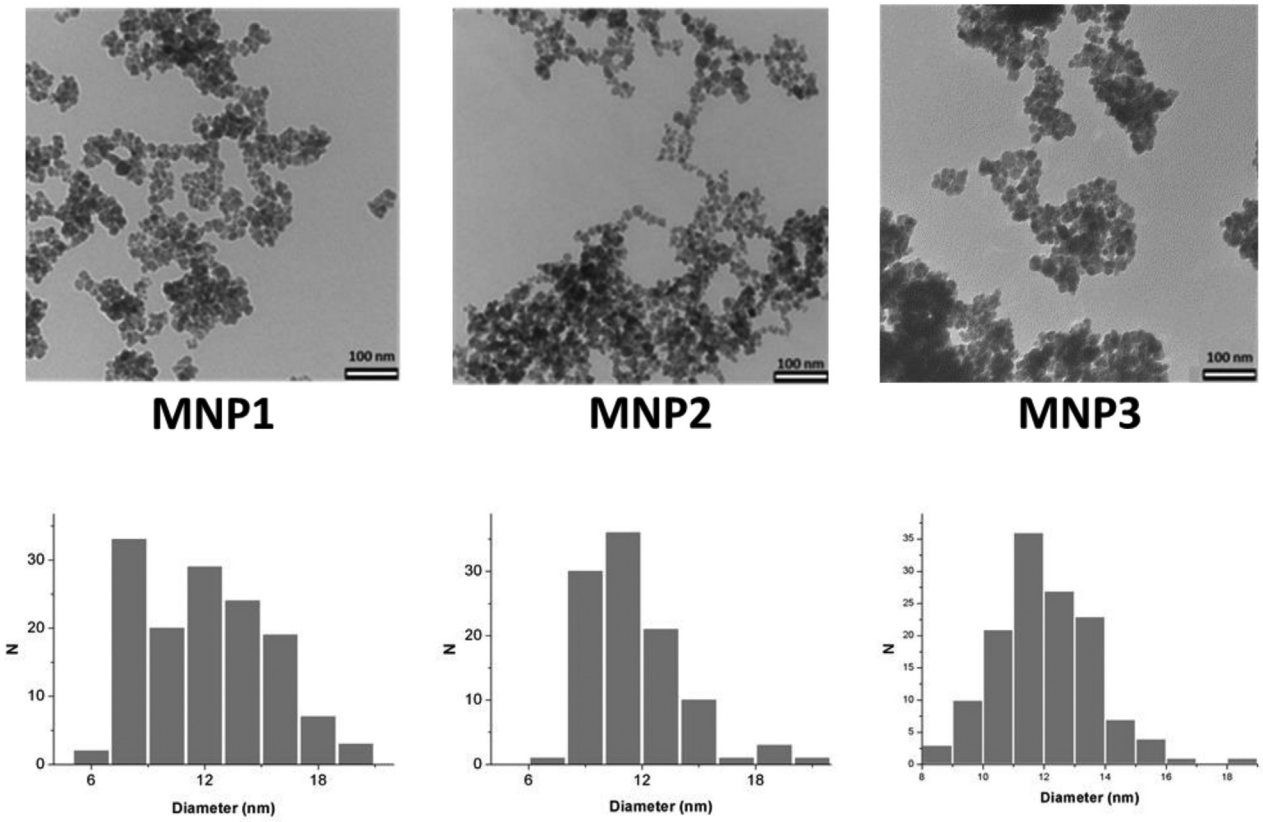

Fig. 2. TEM image and size distribution histogram associated to **MNP1–3**.

supernatant of the reaction was separated under inert atmosphere and mixed with unmodified Fe_3O_4 MNP. In this case, the amount of Fe_3O_4 was reduced by the percentage that there was reacted previously, according to TGA data. This process was repeated several times and subsequent TGA of the new batches of modified MNP showed similar values to those previously obtained. In fact, the whole batches of each type of modified MNP can be mixed for a final characterization process, which showed similar data to those discussed above. Anyway, for the bacteria assays explained below, we have used the MNP produced in the first batch.

3.2. Evaluation of the capacity of MNPs@$G_n(SNMe_3^+)_m$ to capture bacteria

The functionalized **MNP1–3** with cationic ammonium groups make these systems a great candidate to capture and remove different type of bacteria from contaminated media. Our research group has studied the antibacterial activity of CBS dendritic systems functionalized with ammonium groups, being non-selective to interact with Gram-positive and Gram-negative bacteria. For this reason, the first goal was compare the capacity to capture different bacteria strains, *E. coli* (Gram-negative) y *S. aureus* (Gram-positive) with MNP functionalized with different ammonium CBS dendritic systems (**MNP1–3**). The concentration of microorganism used, in each treatment, was 10^8 CFU/ml (colony forming unit). For the MNP, six different concentrations were measured. The methodology used for magnetic separation has five easy steps (Fig. 4): i) Bacteria suspension (10^8 CFU/ml) is mixed with MNP suspension (final concentrations 62.5–2000 ppm); ii) magnetic capture of MNP/bacteria systems; (iii) OD measurement of supernatant; iv) washed of MNP/bacteria systems and v) survival assessment of the bacteria captured by MNP.

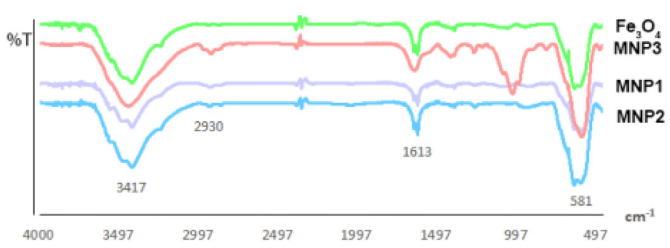

Fig. 3. FTIR spectra of MNP ((MNPs@G_n(S-NMe_3^+)$_m$ (n = 2, m = 4 (**MNP1**); n = 3, m = 8 (MNP**2**)) and MNPs@G_1(S-NMe_3^+)$_7$) (**MNP3**)).

A preliminary assay was done with unmodified MNP, that is, without any dendritic system on their surface, which showed no bacteria capture at all in the range of the concentrations employed. On the other hand, functionalized MNP with CBS dendrons (**MNP1–2**) showed increase efficacy capturing both types of bacteria with increasing concentration (Fig. 5). For Gram-negative model bacteria (*E. coli*), the same tendency was observed for both **MNP1** and **MNP2**. However, the capture of the Gram-positive model bacteria (*S. aureus*) was dependent on dendron generation at lower concentrations. **MNP1**, covered with G2 dendrons, trapped a high percentage of bacteria (> 90%) with concentrations over 1000 ppm,

Table 1
Physical and chemical data obtained for MNP (**MNP1–3**).

	Molar ratio Fe_3O_4/L[a]		D_n^b	%L[c]	N_L^d	N_{func}^e	ρ_{func}^f	ZP[g]
	Theo.	Obt.						
MNP1	1:1	42:1	11	10.2	224	896	2.36	+29.1
MNP2	1:1	34:1	11	21.5	274	2190	5.76	+29.7
MNP3	1:1	149:1	12	6.7	83	579	1.27	+26

a) Molar ratio obtained by TGA, L = dendritic system (Theo. theoretical; Obt. obtained); b) Diameter (nm) obtained by TEM; c) Percentage of organic matter obtained by TGA (%), corresponding with dendritic system coating; d) Number of dendritic systems per MNP; e) Number of functions per MNP; f) Number of functions per nm^2 on MNP surface (N_{func}/nm^2); g) Z potential in mV.

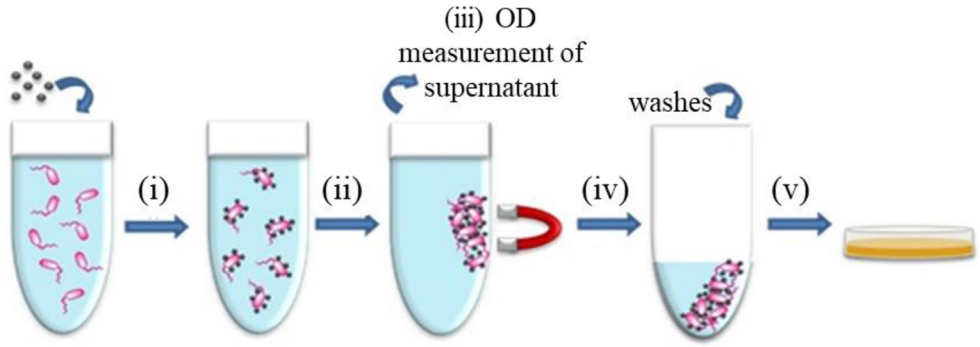

Fig. 4. Methodology followed to capture different bacteria with cationic MNP. i) Bacteria suspension (10^8 CFU/ml) is mixed with MNP suspension (final concentrations 62.5–2000 ppm); ii) magnetic capture of MNP/bacteria systems; (iii) OD measurement of supernatant; iv) washed of MNP/bacteria systems and v) survival assessment of the bacteria capture by MNP.

whereas for **MNP2**, covered with G3 dendrons, this percentage was achieved with a concentration four times lower (250 ppm).

Regarding **MNP3**, covered with G1 CBS dendrimers, a striking difference was observed in its ability to capture bacteria with respect to **MNP1** and **MNP2**. No activity was obtained for *E. coli* at any of the concentrations studied, whereas for *S. aureus* was even slightly more active at low concentrations (88–85%, at 125 ppm and 62.5 ppm, respectively) than **MNP2**.

These results can be justified considering, on one side, the differences between the outer layers of both types of bacteria, and on the other side, the density of active functions, cationic -NMe_3^+ groups, on the surface of **MNP1–3** and the size of the dendritic system that coats these MNP. The outer layer in Gram-negative bacteria is formed by a lipopolysaccharide membrane, while in Gram-positive bacteria is formed by a peptidoglycan layer with embedded teichoic acids. Although both of these layers are negatively charged, the lipopolysaccharide layer of *E. coli* is more negative than the peptidoglycan layer of *S. aureus* [50,51]. The density of cationic groups is clearly lower for **MNP3**, covered with G1 dendrimer, and this MNP was not able to capture Gram-negative *E. coli* bacteria. Due to these facts, we

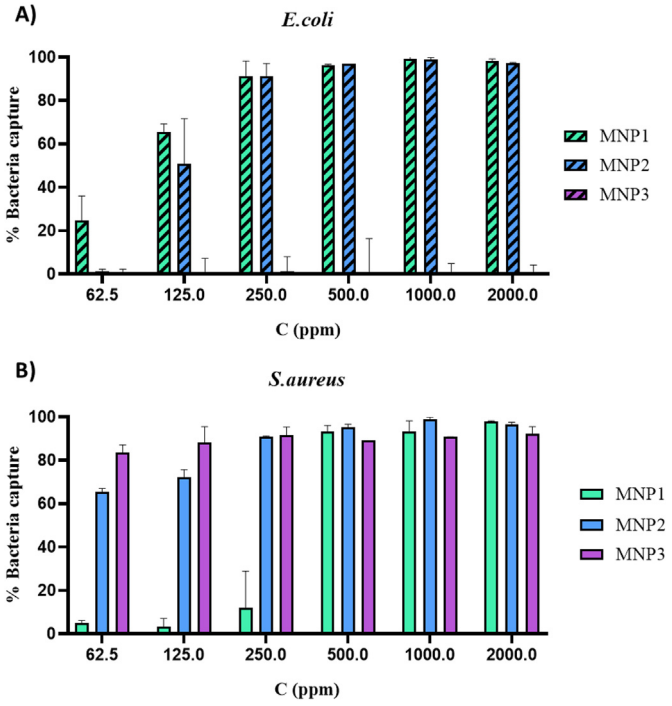

Fig. 5. Percentage (%) of bacteria capture (*E. coli*, (A); *S. aureus*, (B)) with MNPs@G_n(S-NMe_3^+)$_m$ (n = 2, m = 4 (**MNP1**); n = 3, m = 8 (**MNP2**)) and MNPs@G_1(S-NMe_3^+)$_7$ (**MNP3**).

believe that interaction of modified **MNP1–3** bacteria is more dependent on the density of cationic groups on MNP surface. Then, **MNP3** is not able to stablish an interaction strong enough with bacteria to retire them from the suspension. Regarding capture of Gram-positive *S. aureus* bacteria, although the three MNP were able to trap them, at the lowest concentrations studied **MNP2** and **MNP3** were more efficient. These MNP are covered with the biggest dendritic systems, while **MNP1** are covered with smaller G2 dendrons. The smaller size of this dendron entails that it spreads out of the MNP surface to a lesser extent, making more difficult the interaction of the dendrons on **MNP1** with the bacteria wall. Then, at the lowest concentration the interaction can be dependent of the ability of the dendritic systems to generate hydrophobic interactions between the dendritic framework and *S. aureus* bacteria [52]. However, at higher concentrations apparently the density of the cationic groups can compensate the smaller size of G2 dendrons in **MNP1**. Finally, unmodified MNP are not able to retire bacteria from the water suspension because the lack of positive charge on these MNP prevents the establishment of electrostatic interaction with bacteria.

The survival of bacteria captured by MNP was assessed by inoculation of each sample in a Petri dishes containing Muller-Hinton agar (PCA) and incubation at 37 °C for 20 h. In the case of the MNPs/bacteria systems, microbial growth was observed for all the concentrations used. These results showed that **MNP1–3** captured bacteria, but they were able to survive, even at high concentrations of MNP. An analogous procedure was followed for the supernatants of the bacteria capture treatments. The inoculum corresponding with the samples that showed better capture (over 99%) did not show microbial growth.

The systems **MNP1–3**/bacteria formed at higher concentration of MNP (capture ca. 100%) during the interaction were isolated from the suspensions with the magnet and were analyzed by TEM (*S. aureus* Figs. 6A-C, *E. coli* Figs. 6D-E). The pictures showed that MNP wrapped completely bacteria. Similarly, the images obtained by SEM allowed us to observe the treated bacteria (*S. aureus* Fig. 6F-H, *E. coli* Figs. 6I-J).

3.3. Capture of S. aureus and E. coli at low bacteria concentration

Since **MNP2**, dendronized with G3 CBS dendrons, presented higher capacity to interact with both bacteria than **MNP1** and **MNP3**, even at low concentration, they were selected for the following experiments.

In order to study the capture limit of *S. aureus* and *E. coli*, at ultralow concentrations, a wide range of bacteria concentrations have been analyzed (10^8–10^3 CFU/ml), mixing with **MNP2** (500 ppm final concentration for all samples). Bacteria capture process was carried out as previously was describe, but in this case, the percentage of bacteria capture and the toxicity of each treatment was obtained by counting colonies of bacteria in PCA-agar plates. Controls for each bacteria concentration, as well as all supernatants and bacteria/**MNP2** aggregates were seeded in PCA-agar plates and incubated at 37 °C for 20 h.

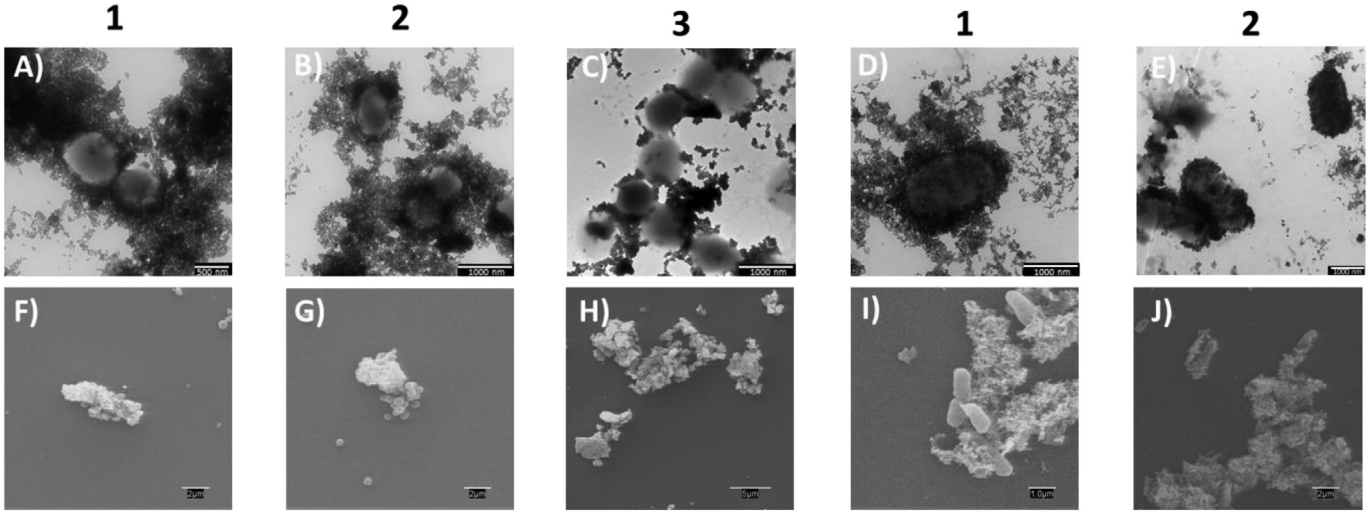

Fig. 6. TEM images of the interaction between MNP **MNP1–3** with *S. aureus* (A-C) and *E. coli* (D-E); SEM images of the interaction between **MNP1–3** with *S. aureus* (F-H) and *E. coli* (I-J).

Results obtained for each supernatant showed no colonies growing, meaning a total bacteria capture, even at ultralow concentration (Fig. 7A). Additionally, this methodology allowed knowing the viability of the bacteria after being trapped with cationic **MNP2** at low bacteria concentration (Fig. 7B). As can be seen, the decreasing of bacteria concentration led to **MNP2** to significantly become more bactericide, that is, **MNP2** removed most of the bacteria present in the medium and also kill them. This behavior can be related with the presence of excess positive charges, since these dendritic systems and NP modified with them have shown bactericidal properties [43,45,46].

3.4. Recovery and reuse of MNP2 (MNP@G3(S-NMe_3^+)$_8$)

The capacity to recovery and reuse **MNP2** for successive water purification cycles was assessed by two different processes. First, we analyzed how many times could be used the **MNP2** without any treatment between cycles. For that, **MNP2** at the concentrations used (1000, 500, 250 ppm) were mixed three times with *E. coli* and *S. aureus* (10^8 CFU/ml). The results (Fig. 8) showed that bacteria capture decreased for each repetition. This was more notably as the concentration of **MNP2** diminished, meaning that saturation of MNP was reached before, as expected. In addition, **MNP2** exhibited better potential to be reused with *S. aureus* (Fig. 8B) than with *E. coli* (Fig. 8A), confirming the behavior discussed above about bacteria capture at low concentrations.

Second, the other procedure consisted on washing with an ethanol/water solution (75/25 *v*/v) the **MNP2**/bacteria aggregates after each bacteria capture cycle; with the aim to remove bacteria from the MNP surface. However, this procedure worsened the results with respect to the previous assay without this washing (Fig. 8). In this treatment, **MNP2** dispersed more difficultly in the ethanol/water mixture and consequently these MNP kept higher level of aggregation, thus reducing the amount of available surface to interact with bacteria. Furthermore, the ethanol/water mixture denatured bacteria and their components released to the mixture, which probably will interact electrostatically with the MNP surface, blocking their ability to capture bacteria.

4. Conclusions

Cationic MNP grafted with cationic CBS dendritic systems are easily prepared by reaction between unmodified MNP and the corresponding cationic CBS dendrons and dendrimers containing one triethoxysilyl moiety, at the focal point in dendrons and at the periphery in dendrimers. The functionalization degree of these modified MNP (**MNP1–3**) is clearly dependent on the topology of the dendritic compounds, being more favorable the reaction for CBS dendrons than for CBS dendrimers due to that the triethoxysilyl moiety is more achievable in the first type of compounds than in the second.

The ability to trap bacteria with these cationic **MNP1–3** has been explored for a model of Gram-positive (*S. aureus*) and Gram-negative (*E. coli*) bacteria. The results were affected by size of dendritic system grafting the MNP surface, density of ammonium groups on MNP surface and type of bacteria (Gram-positive vs. Gram-negative). The best

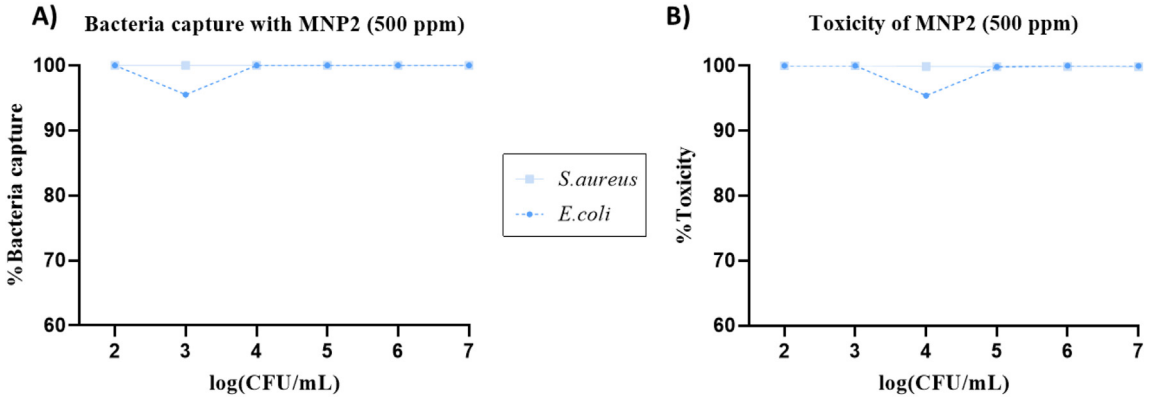

Fig. 7. A) Percentage (%) of bacteria capture at different bacteria concentrations (10^7–10^2 CFU/ml) with **MNP2** (500 ppm of MNP@G3(NMe_3^+)$_8$); B) Study of the bacteria viability at different bacteria concentrations (10^7–10^2 CFU/ml) after being capture by **MNP2** (500 ppm of MNP@G3(NMe_3^+)$_8$).

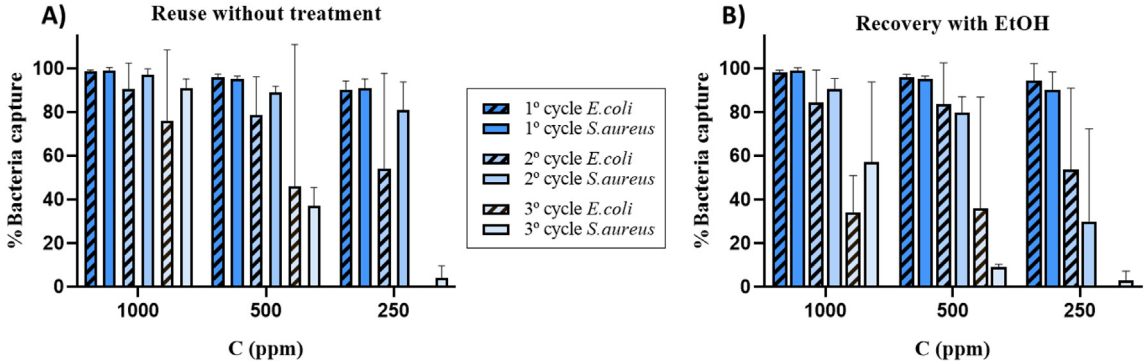

Fig. 8. Analysis of the capacity to reuse **MNP2** at different concentrations for three cycles: A) without treatment and B) with EtOH washing.

interaction with *E. coli* was performed by MNP covered with higher density of cationic groups, that is **MNP1** and **MNP2**, grafted with dendrons, as consequence of the general higher affinity of Gram-negative bacteria toward cationic charges due to their coating with lipopolysaccharide molecules, which carry a negative charge. Regarding *S. aureus* capture, the most efficient systems were **MNP2** and **MNP3**, which were modified with the biggest groups, G3 dendron and G1 dendrimer respectively, favouring their approach to the bacteria surface.

The reuse of these MNP for several cycles of bacteria capture was limited by the adsorption of bacteria on the MNP surface, which is related with the amount of cationic groups on the surface. Hence, **MNP2** with highest ammonium density could be used three times for bacteria capture, whereas the other two MNP were only effective for two cycles.

In the view of these results and considering the amount of MNP to remove bacteria, these systems could be considered as purification systems for small amounts of water or as models to study the interaction of bacteria with different ligands. Further studies to improve the results with different bacteria or to translate them to other materials are being carried out.

Authors statement

Conceptualization, J.S.-N., R.G., F.J.d.l.M. and J.L.C.-P.; methodology, S.Q., A.B.G., J.S.-N., J.L.C.P.; investigation, S.Q., A.B.G.; writing—original draft preparation, S.Q., A.B.G., J.S.-N.; writing—review and editing, S.Q., J.S.N.; supervision, J.S.-N., F.J.d.l.M.; project administration, R.G., F.J.d.l.M.; funding acquisition, R.G., F.J.d.l.M., J.S.N. All authors have read and agreed to the published version of the manuscript.

Declaration of Competing Interest

The authors declare no conflict of interest.

Acknowledgments

This work has been supported by grants from PID2020-112924RB-I00 (MINECO), Consortiums NANODENDMED II-CM ref. B2017/BMD-3703 and IMMUNOTHERCAN-CM B2017/BMD-3733 (CAM) to UAH and grant EPU-INV/2020/014 (CAM, UAH). CIBER-BBN is an initiative funded by VI National R-D-i Plan 2008-2011, Iniciativa Ingenio 2010, Consolider Program, CIBER Actions and financed by the Instituto de Salud Carlos III with assistance from the European Regional Development Fund. S.Q.S. acknowledges UAH for a predoctoral fellowship.

References

[1] Progress on Household Drinking Water, Sanitation and Hygiene 2000-2020: Five Years into the SDGs, World Health Organization (WHO) and the United Nations Children's Fund (UNICEF), Geneva, 2021.
[2] V. Economou, P. Gousia, Agriculture and food animals as a source of antimicrobial-resistant bacteria, Infect. Drug Resist. 8 (2015) 49–61.
[3] C. Manyi-Loh, S. Mamphweli, E. Meyer, A. Okoh, Antibiotic use in agriculture and its consequential resistance in environmental sources: potential public health implications, Molecules 23 (2018) 79.
[4] P.J.J. Alvarez, C.K. Chan, M. Elimelech, N.J. Halas, D. Villagrán, Emerging opportunities for nanotechnology to enhance water security, Nat. Nanotechnol. 13 (2018) 634–641.
[5] S. Chaturvedia, P.N. Dave, Water purification using nanotechnology an emerging opportunities, Chem. Methodol. 3 (2019) 115–144.
[6] A. Akbarzadeh, M. Samiei, S. Davaran, Magnetic nanoparticles: preparation, physical properties, and applications in biomedicine, Nanoscale Res. Lett. 7 (2012) 144.
[7] C.M. Earhart, C.E. Hughes, R.S. Gaster, C.C. Ooi, R.J. Wilson, L.Y. Zhou, E.W. Humke, L. Xu, D.J. Wong, S.B. Willingham, E.J. Schwartz, I.L. Weissman, S.S. Jeffrey, J.W. Neal, R. Rohatgi, H.A. Wakelee, S.X. Wang, Isolation and mutational analysis of circulating tumor cells from lung cancer patients with magnetic sifters and biochips, LabChip 14 (2014) 78–88.
[8] C. Marquina, J.M. de Teresa, D. Serrate, J. Marzo, F.A. Cardoso, D. Saurel, S. Cardoso, P.P. Freitas, M.R. Ibarra, GMR sensors and magnetic nanoparticles for immunochromatographic assays, J. Magn. Magn. Mater. 324 (2012) 3495–3498.
[9] S.C. McBain, H.H.P. Yiu, J. Dobson, Magnetic nanoparticles for gene and drug delivery, Int. J. Nanomed. 3 (2008) 169–180.
[10] M. Pernia Leal, S. Rivera-Fernandez, J.M. Franco, D. Pozo, J.M. de la Fuente, M.L. Garcia-Martin, Long-circulating PEGylated manganese ferrite nanoparticles for MRI-based molecular imaging, Nanoscale 7 (2015) 2050–2059.
[11] A.N.M.P. Oksvold, K.W. Pedersen, Magnetic bead-based isolation of exosomes, Methods Mol. Biol. 1218 (2015) 465–481.
[12] M.S.I. Safarik, Magnetic techniques for the isolation and purification of proteins and peptides, Biomagn. Res. Technol. 2 (2004) 7.
[13] M.I. Din, A.G. Nabi, Z. Hussain, M. Arshad, A. Intisar, A. Sharif, E. Ahmed, H.A. Mehmood, M.L. Mirza, Innovative seizure of Metal/Metal oxide nanoparticles in water purification: a critical review of potential risks, Crit. Rev. Anal. Chem. 49 (2019) 534–541.
[14] Y.-W. Choi, H. Lee, Y. Song, D. Sohn, Colloidal stability of iron oxide nanoparticles with multivalent polymer surfactants, J. Colloid Interface Sci. 443 (2015) 8–12.
[15] I.W. Hamley, Nanotechnology with soft materials, Angew. Chem. Int. Ed. 42 (2003) 1692–1712.
[16] M.N. Ghazzal, J. Goffin, E.M. Gaigneaux, Y. Nizet, Magnetic nanoparticle with high efficiency for bacteria and yeast extraction from contaminated liquid media, J. Taiwan Inst. Chem. Eng. 71 (2017) 62–68.
[17] A. Barrios-Gumiel, D. Sepúlveda-Crespo, J.L. Jiménez, R. Gómez, M.Á. Muñoz-Fernández, F.J. de la Mata, Dendronized magnetic nanoparticles for HIV-1 capture and rapid diagnostic, Colloids Surf B Biointerfaces 181 (2019) 360–368.
[18] D. Zhang, J.P. Berry, D. Zhu, Y. Wang, Y. Chen, B. Jiang, S. Huang, H. Langford, G. Li, P.A. Davison, J. Xu, E. Aries, W.E. Huang, Magnetic nanoparticle-mediated isolation of functional bacteria in a complex microbial community, ISME J. 9 (2015) 603–614.
[19] H. Lee, H. Han, S. Jeon, Baleen-mimicking virtual filters for rapid detection of pathogenic bacteria in water using magnetic nanoparticle chains and a halbach ring, ACS Sensors 5 (2020) 3432–3437.
[20] Z. Li, J. Ma, J. Ruan, X. Zhuang, Using positively charged magnetic nanoparticles to capture bacteria at ultralow concentration, Nanoscale Res. Lett. 14 (2019) 195.
[21] Z.Q. Shi, L.Q. Jin, C. He, Y.P. Li, C.J. Jiang, H. Wang, J. Zhang, J.X. Wang, W.F. Zhao, C.S. Zhao, Hemocompatible magnetic particles with broad-spectrum bacteria capture capability for blood purification, J. Colloid Interface Sci. 576 (2020) 1–9.
[22] Y. Zhu, C. Xu, N. Zhang, X. Ding, B. Yu, F.-J. Xu, Polycationic synergistic antibacterial agents with multiple functional components for efficient anti-infective therapy, Adv. Funct. Mater. 28 (2018) 1706709.
[23] H. Liu, Y. Hu, Y. Zhu, X. Wu, X. Zhou, H. Pan, S. Chen, P. Tian, A simultaneous grafting/vinyl polymerization process generates a polycationic surface for enhanced antibacterial activity of bacterial cellulose, Int. J. Biol. Macromol. 143 (2020) 224–234.
[24] M.-M. Zhu, Y. Fang, Y.-C. Chen, Y.-Q. Lei, L.-F. Fang, B.-K. Zhu, H. Matsuyama, Antifouling and antibacterial behavior of membranes containing quaternary ammonium and zwitterionic polymers, J. Colloid Interf. Sci. 584 (2021) 225–235.
[25] A. Muñoz-Bonilla, M. Fernández-García, Polymeric materials with antimicrobial activity, Prog. Polym. Sci. 37 (2012) 281–339.
[26] D.A. Tomalia, J.M.J. Fréchet, Discovery of dendrimers and dendritic polymers: a brief historical perspective, J. Polym. Sci. Part A Polym. Chem. 40 (2002) 2719–2728.

[27] A. Carlmark, C. Hawker, A. Hult, M. Malkoch, New methodologies in the construction of dendritic materials, Chem. Soc. Rev. 38 (2009) 352–362.
[28] M. Malkoch, S. García-Gallego, Monographs in Supramolecular Chemistry, Dendrimer Chemistry: Synthetic Approaches Towards Complex Architectures, Royal Society of Chemistry, 2020.
[29] E. Fuentes-Paniagua, J.M. Hernández-Ros, M. Sánchez-Milla, M.A. Camero, M. Maly, J. Pérez-Serrano, J.L. Copa-Patiño, J. Sánchez-Nieves, J. Soliveri, R. Gómez, F.J. de la Mata, Carbosilane cationic dendrimers synthesized by thiol-ene click chemistry and their use as antibacterial agents, RSC Adv. 4 (2014) 1256–1265.
[30] E.J. Ramchuran, I. Pérez-Guillén, L.A. Bester, R. Khan, F. Albericio, M. Viñas, B.G. de la Torre, Super-cationic peptide Dendrimers—synthesis and evaluation as antimicrobial agents, Antibiotics 10 (2021) 695.
[31] A.M. Schito, G.C. Schito, S. Alfei, Synthesis and antibacterial activity of cationic amino acid-conjugated dendrimers loaded with a mixture of two triterpenoid acids, Polymers 13 (2021) 521.
[32] K. Ciepluch, B. Maciejewska, K. Gałczyńska, D. Kuc-Ciepluch, M. Bryszewska, D. Appelhans, Z. Drulis-Kawa, M. Arabski, The influence of cationic dendrimers on antibacterial activity of phage endolysin against P. Aeruginosa cells, Bioorg. Chem. 91 (2019), 103121.
[33] I. Pakrudheen, A.N. Banu, E. Murugan, Cationic amphiphilic dendrimers with tunable hydrophobicity show in vitro activity, Environ. Chem. Lett. 16 (2018) 1513–1519.
[34] H.W. VanKoten, W.M. Dlakic, R. Engel, M.J. Cloninger, Synthesis and biological activity of highly cationic dendrimer antibiotics, Mol. Pharm. 13 (2016) 3827–3834.
[35] S. Mignani, X. Shi, V. Ceña, J. Rodrigues, H. Tomas, J.-P. Majoral, Engineered non-invasive functionalized dendrimer/dendron-entrapped/complexed gold nanoparticles as a novel class of theranostic (radio)pharmaceuticals in cancer therapy, J. Control. Release 332 (2021) 346–366.
[36] G. Jiang, S. Liu, T. Yu, R. Wu, Y. Ren, H.C. van der Mei, J. Liu, H.J. Busscher, PAMAM dendrimers with dual-conjugated vancomycin and ag-nanoparticles do not induce bacterial resistance and kill vancomycin-resistant staphylococci, Acta Biomater. 123 (2021) 230–243.
[37] Q.X. Zhou, Y.L. Wu, Y. Sun, X.Y. Sheng, Y.Y. Tong, J.H. Guo, B.Y. Zhou, J.Y. Zhao, Magnetic polyamidoamine dendrimers for magnetic separation and sensitive determination of organochlorine pesticides from water samples by high-performance liquid chromatography, J. Environ. Sci. 102 (2021) 64–73.
[38] X.Y. Feng, X.Y. Meng, F.B. Xiao, Z.P. Aguilar, H.Y. Xu, Vancomycin-dendrimer based multivalent magnetic separation nanoplatforms combined with multiplex quantitative PCR assay for detecting pathogenic bacteria in human blood, Talanta 225 (2021).
[39] S. Singh, D. Bahadur, Highly efficient and reusable dendritic Fe3O4 magnetic nanoadsorbent for inhibition of bacterial growth, Surf. Interfaces 17 (2019), 100348.
[40] M.H. Beyki, J. Malakootikhah, F. Shemirani, S. Minaeian, Magnetic CoFe2O4@ melamine based hyper-crosslinked polymer: a multivalent dendronized nanostructure for fast bacteria capturing from real samples, Process Safe Environ. Prot. 116 (2018) 14–21.
[41] P. Ortega, J. Sánchez-Nieves, J. Cano, R. Gómez, F.J. de la Mata, Poly(carbosilane) dendrimers and other silicon-containing dendrimers, dendrimer chemistry: synthetic approaches towards complex architectures, R. Soc. Chem. 5 (2020) 120–151.
[42] I. Heredero-Bermejo, J.M. Hernandez-Ros, L. Sanchez-Garcia, M. Maly, C. Verdu-Exposito, J. Soliveri, F.J. de la Mata, J.L. Copa-Patino, J. Perez-Serrano, J. Sanchez-Nieves, R. Gomez, Ammonium and guanidine carbosilane dendrimers and dendrons as microbicides, Eur. Polym. J. 101 (2018) 159–168.
[43] E. Fuentes-Paniagua, J. Sánchez-Nieves, J.M. Hernández-Ros, A. Fernández-Ezequiel, J. Soliveri, J.L. Copa-Patiño, R. Gómez, F.J. de la Mata, Structure-activity relationship study of cationic carbosilane dendritic systems as antibacterial agents, RSC Adv. 6 (2016) 7022–7033.
[44] M. Sánchez-Milla, R. Gómez, J. Pérez-Serrano, J. Sánchez-Nieves, F.J. de la Mata, Functionalization of silica with amine and ammonium alkyl chains, dendrons and dendrimers: synthesis and antibacterial properties, Mater. Eng. Sci. C (2020) 110526.
[45] A. Barrios-Gumiel, J. Sánchez-Nieves, J. Péez-Serrano, R. Gómez, F.J. de la Mata, PEGylated AgNP covered with cationic carbosilane dendrons to enhance antibacterial and inhibition of biofilm properties, Int. J. Pharm. 569 (2019).
[46] C.E. Peña-Gonzalez, E. Pedziwiatr-Werbicka, T. Martín-Pérez, E.M. Szewczyk, J.L. Copa-Patiño, J. Soliveri, J. Pérez-Serrano, R. Gómez, M. Bryszewska, J. Sánchez-Nieves, F.J. de la Mata, Antibacterial and antifungal properties of dendronized silver and gold nanoparticles with cationic carbosilane dendrons, Int. J. Pharm. 528 (2017) 55–61.
[47] M. Sánchez-Milla, R. Gómez, J. Pérez-Serrano, J. Sánchez-Nieves, F.J. de la Mata, Functionalization of Silica with Amine and Ammonium Alkyl Chains, Dendrons and Dendrimers: Synthesis and Antibacterial Properties, 109, 2020, p. 110526.
[48] S. Quintana-Sánchez, Ph. D. Thesis, University of Alcala, 2021.
[49] R. Khodadust, G. Unsoy, S. Yalcın, G. Gunduz, U. Gunduz, PAMAM dendrimer-coated iron oxide nanoparticles: synthesis and characterization of different generations, J. Nanopart. Res. 15 (2013) 1488.
[50] Y.N. Slavin, J. Asnis, U.O. Häfeli, H. Bach, Metal nanoparticles: understanding the mechanisms behind antibacterial activity, J. Nanobiotechnol. 15 (2017) 65.
[51] M.N. Sonohara, H. Ohshima, T. Kondo, Difference in surface properties between Escherichia coli and Staphylococcus aureus as revealed by electrophoretic mobility measurements, Biophys. Chem. 55 (1995) 273–277.
[52] F. Figueredo, A. Saavedra, E. Cortón, V.E. Diz, Hydrophobic forces are relevant to bacteria-nanoparticle interactions: pseudomonas putida capture efficiency by using arginine, cysteine or oxalate wrapped magnetic nanoparticles, Colloids Interf. 2 (2018) 29.